

Research Report  
UKTRP-82-24

ENGINEERING PROPERTIES OF OVERBURDEN MATERIALS  
FOR THE MEANS PROJECT

by

---

Vincent P. Drnevich  
Chairman, Department of Civil Engineering

David L. Allen  
Kentucky Transportation Research Program

and

Tommy C. Hopkins  
Kentucky Transportation Research Program

College of Engineering  
University of Kentucky

---

December 1982

## INTRODUCTION

A geotechnical investigation was performed to determine the physical properties (classification) and engineering properties of the overburden material from a proposed oil shale mining site in Montgomery County (Means Project). Three overburden materials were recieved in sealed metal drums and were labeled Nancy Member, Borden Formation; Clay City Bed, Farmers Member, Borden Formation; and Henley bed, Farmers Member, Borden Formation. Hereafter, they will be referred to as the Nancy, Clay City and Henley, respectively. The various types of geotechnical laboratory tests performed on these materials are listed in Table 1.

## PHYSICAL PROPERTIES

The natural moisture contents of all the materials were obtained. The materials, as recieved that were too large to test were run through a crusher until all particles passed the 3/4-inch sieve. Liquid and plastic limit tests were performed on the materials according to ASTM D 423-66 and ASTM D 424-59. The specific gravity of the soil solids were determined according to ASTM D 854-58. Results of the limits and specific gravity tests and natural moisture contents are summarized in Table 2. Particle-size analysis was determined according to ASTM D 422-63. Particle-size distribution for these materials are shown in Figure 1.

## ENGINEERING PROPERTIES

Standard compaction tests were performed on the three

materials according to ASTM D 698-70, Method A (compactive effort= 12,730 ft.-lb./ft<sup>3</sup>) The results are shown in Figure 2, and are summarized in Table 3. To approximate the conditions under which these materials might be placed in the field, an additional moisture-density point was performed on each of the materials at the natural moisture content. The results of these three additional points are listed in Table 3.

To determine the effective stress parameters that are used to evaluate the stability of compacted embankments, three isotropically consolidated-drained triaxial tests were performed on each of the three materials. The triaxial specimens were compacted at natural moisture contents to the densities listed in column 4 of Table 3. The specimens were four inches in diameter and eight inches in height. These dimensions limited the largest particle size to 3/4-inch. Filter paper strips were mounted along side of each specimen to permit faster drainage of the pore fluid, thus preventing a build-up of pore pressures during shear.

When performing a consolidated-drained triaxial test, it is essential that accurate readings of the volume change of the specimen be obtained during the test. If the specimen is not saturated or if air bubbles are present in the drainage lines, improper volume change readings will occur. To facilitate saturation, the specimen and drainage lines were evacuated of air by vaccuuming and then allowing water, under back pressure, to fill the voids. After saturation,

the specimen was allowed to consolidate to the desired effective stress for a minimum of 24 hours.

During the test, a pore pressure transducer was connected to the top drainage line. This was monitored to determine if positive pore pressures were building up in the specimen. If positive pore pressures began to build up, then the strain rate was reduced to allow the pressures to dissipate. The bottom drainage line was connected to a burette from which the volume change was monitored throughout the test. A summary of the triaxial testing conditions is given in Table 4.

The results of the triaxial tests are illustrated in figures 3 through 5. the internal friction angle,  $\bar{\phi}$ , for the Nancy material (Figure 3) was  $27.3^\circ$  and the cohesion value was zero. The failure envelopes for the Henley and Clay City materials curved downward, possibly due to particle crushing at higher confining pressures. This is similar to data reported by Marsal(1). For the test data associated with these two materials equivalent sets of cohesion,  $\bar{c}_e$ , and friction angle,  $\bar{\phi}_e$ , were determined by fitting the curved  $K_f$  -lines in Figures 4 and 5 with a hyperbolic function of the following form:

$$q_f = \bar{p} / (b\bar{p}_f + c)$$

where  $q_f$  = maximum deviator stress at failure

$\bar{p}_f$  = maximum effective normal stress at failure and

$b, c$  = constants.

The tangent to the curve at any point is obtained from the

first derivative,

$$dq_f / d\bar{p}_f = (c) / (b^2 \bar{p}_f^2 + 2bc\bar{p}_f + c^2) = \tan \alpha$$

The arcsin of the above equation gives  $\bar{\phi}_e$ . Table 5 lists these values of  $\bar{\phi}_e$  for various effective pressures of embankments for Henley and Clay City. The equivalent effective cohesion value,  $\bar{c}_e$ , for any particular  $\bar{p}$  and its associated  $\bar{\phi}_e$ , is defined from the following equation:

$$\bar{c}_e = (\bar{p}_f / (b\bar{p}_f + c) - \tan \alpha \bar{p}_f) / \cos \bar{\phi}_e.$$

The last column of Table 5 lists values of  $\bar{c}_e$ . Values of  $\bar{\phi}_e$  and  $\bar{c}_e$  in Table 5 are equivalent because they provide equivalent values of  $\bar{\phi}$  and  $\bar{c}$  for a given  $\bar{p}_f$  to simulate the curved failure envelope. They are not true values of friction and cohesion.

One-dimensional compression tests were performed on the overburden materials. The test consisted of two different phases. The first phase of testing was designed to determine how the material in a dry state would perform under one-dimensional loading. The purpose of the second phase was to evaluate creep characteristics of the oil shales when inundated with water.

The procedure for the first phase consisted of compacting the shales to dry density at natural moisture content in a 6-inch diameter mold to a height of 2.625 inches. These dimensions were used to minimize the effects of frictional forces acting on the sides of the molds during loading. The specimens were loaded and deformations were recorded in a manner similar to the consolidation tests.

Loads of 1, 2, 3, 4, 8, and 16 tons per square foot were used. For each load when the sample deformed less than .0025 inch in two minutes, the next load was applied.

The strain for each load was calculated by dividing the deformation occurring under each load by the original height of the specimen. The stress-strain curves for the three materials are given in Figure 6.

Creep characteristics of the shales were studied by reloading the previously loaded specimen to 4 tons per square foot. The specimen was allowed to compress for approximately fifteen minutes or until all deformation had stopped. The mold and specimen were inundated in water while the stress level remained constant at 4 tons per square foot. The time required to submerge the specimen was less than five seconds. Upon inundation, a timer was immediately started and deformations and elapsed times were recorded. Strains were calculated by dividing deformations associated with time after inundation by the original specimen height before loading. The strains after inundation were plotted as a function of time as shown in Figure 7. This figure indicates that the Nancy and Henley are highly susceptible to slaking.

#### REFERENCE

1. Hirschfeld, R.C.; and Poulos, S.J.; Embankment-Dam Engineering (Mechanical Properties of Rockfill by Raul J. Marsal), Casagrande Volume, John Wiley and Sons, Inc., New York.

TABLE 1. SUMMARY OF TESTING PROGRAM\*

MATERIAL NAME	NATURAL MOISTURE	SPECIFIC GRAVITY	LIQUID LIMIT	PLASTIC LIMIT	GRAIN SIZE	MOISTURE DENSITY	TRIAXIAL TESTS		
							20 Psi	40 Psi	80 Psi
NANCY	X	X	X	X	X	X	X	X	X
HENLEY	X	X	X	X	X	X	X	X	X
CLAY CITY	X	X	X	X	X	X	X	X	X

\* X- INDICATES TEST WAS PERFORMED

TABLE 2. RESULTS OF PHYSICAL PROPERTIES TESTS.

MATERIAL NAME	NATURAL MOISTURE CONTENTS (%)	SPECIFIC GRAVITY	LIQUID LIMIT	PLASTICITY INDEX
NANCY	7.6	2.75	32.8	10.7
HENLEY	4.5	2.74	27.5	8.5
CLAY CITY	3.5	2.75	-----	NP



TABLE 3. RESULTS OF MOISTURE-DENSITY TESTS.

MATERIAL NAME	OPTIMUM MOISTURE CONTENTS (%) (%)	MAXIMUM DRY DENSITY (lb./ft. <sup>3</sup> )	DENSITY AT NATURAL MOISTURE CONTENT (lb./ft. <sup>3</sup> )
NANCY	14.3	122.9	119.6
HENLEY	10.5	129.6	120.2
CLAY CITY	4.6	116.0	113.8

TABLE 4. SUMMARY OF TRIAXIAL TEST CONDITIONS.

MATERIAL NAME	EFFECTIVE CONFINING PRESSURE (psi)	'B' PORE PRESSURE PARAMETER	AVERAGE STRAIN RATE (in./min.)
NANCY	20	1.00	0.00047
	40	1.00	0.00024
	80	1.00	0.0039
HENLEY	20	0.91	0.00089
	40	1.00	0.00070
	80	0.65	0.0019
CLAY CITY	20	1.00	0.0027
	40	1.00	0.0020
	80	0.40	0.0024

Table 5. VALUES OF  $\bar{\phi}$ ,  $\bar{\phi}_e$ ,  $\bar{c}$ , &  $\bar{c}_e$  FOR VARIOUS PRESSURES.

NANCY				
$\bar{p}_f$ (psi)	$q_f$ (psi)	SIN $\bar{\phi}$	$\bar{\phi}$ (degrees)	$\bar{c}$ (psi)
P R E S S U R E S		.485	27.3	27.3
HENLEY				
$\bar{p}_f$ (psi)	$q_f$ (psi)	SIN $\bar{\phi}$	$\bar{\phi}_e^1$ (degrees)	$\bar{c}_e$ (psi)
10	5.8	.58	35.5	0.0
20	11.5	.57	34.8	0.2
30	17.2	.56	34.0	0.5
40	22.7	.55	33.4	0.9
50	28.2	.54	32.7	1.4
60	33.5	.53	32.0	2.0
70	38.8	.52	31.3	2.8
80	44.0	.5153	31.0	3.4
90	49.1	.507	30.5	4.0
100	54.1	.50	30.0	4.8
110	59.1	.49	29.3	5.9
120	63.9	.48	28.7	7.2
CLAY CITY				
$\bar{p}_f$ (psi)	$q_f$ (psi)	SIN $\bar{\phi}$	$\bar{\phi}_e^1$ (degrees)	$\bar{c}_e$ (psi)
10	7.491	.732	47.1	0.3
20	14.652	.700	44.4	0.9
30	21.505	.671	42.1	1.9
40	28.070	.643	40.0	3.1
50	34.364	.616	38.0	4.5
60	40.404	.592	36.3	6.1
70	46.205	.569	34.7	7.8
80	51.780	.548	33.2	9.5
90	57.143	.526	31.7	11.5
100	62.305	.507	30.5	13.5
110	67.287	.488	29.2	15.6
120	72.072	.471	28.1	17.6

1. Equivalent values to approximate curved failure envelopes.

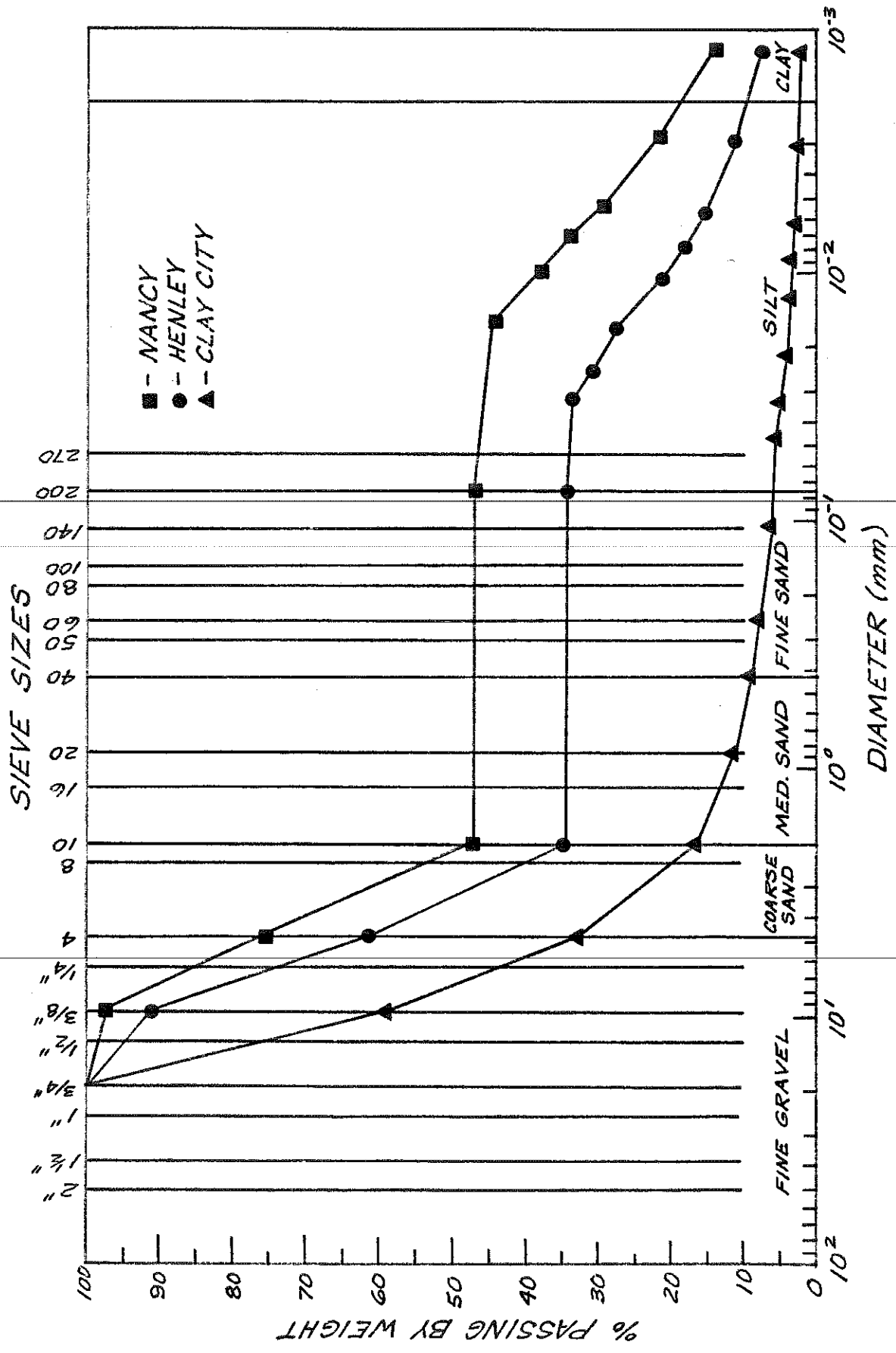


FIGURE 1. GRAIN-SIZE DISTRIBUTIONS.

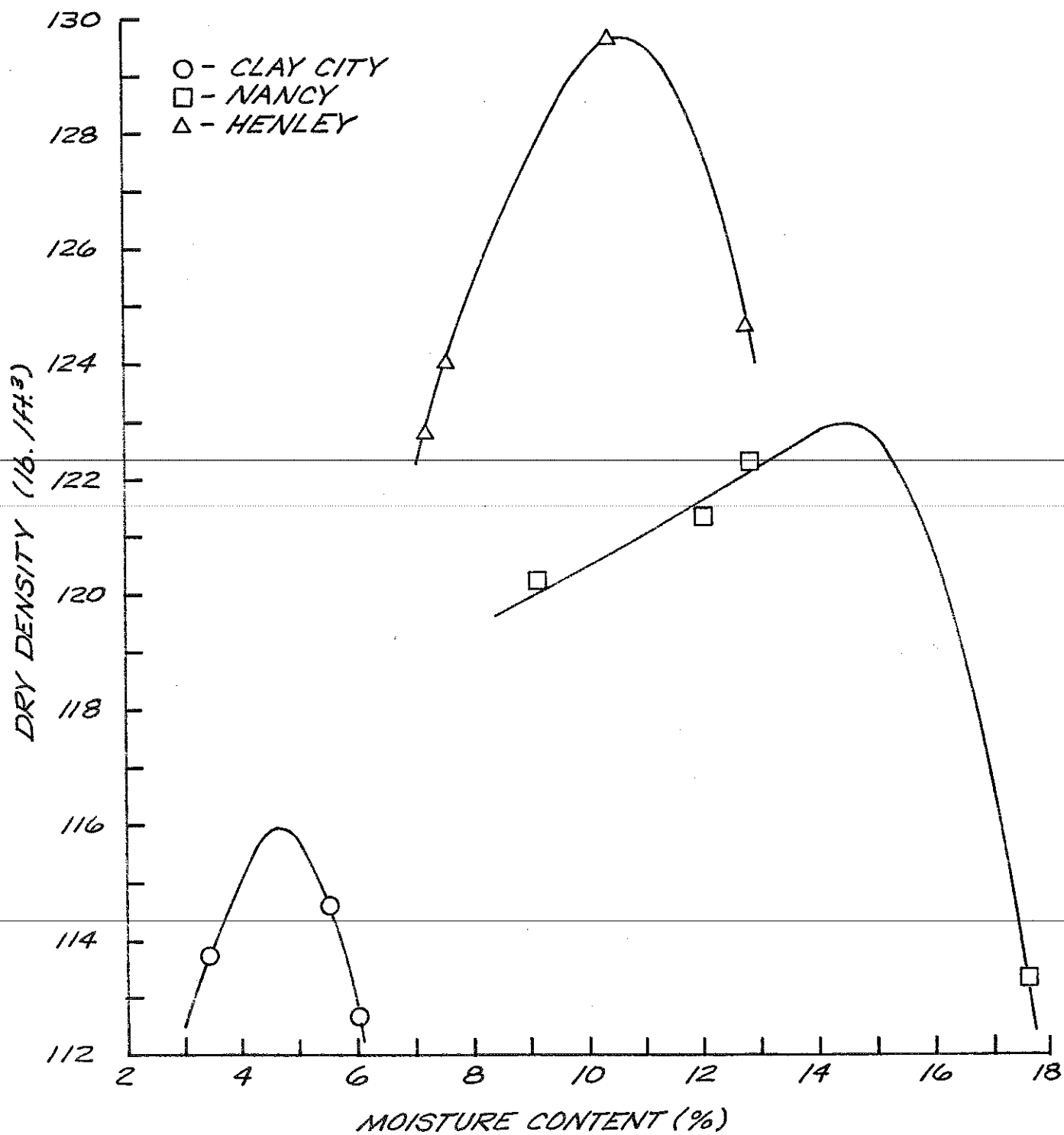


FIGURE 2. MOISTURE-DENSITY RELATIONSHIPS.

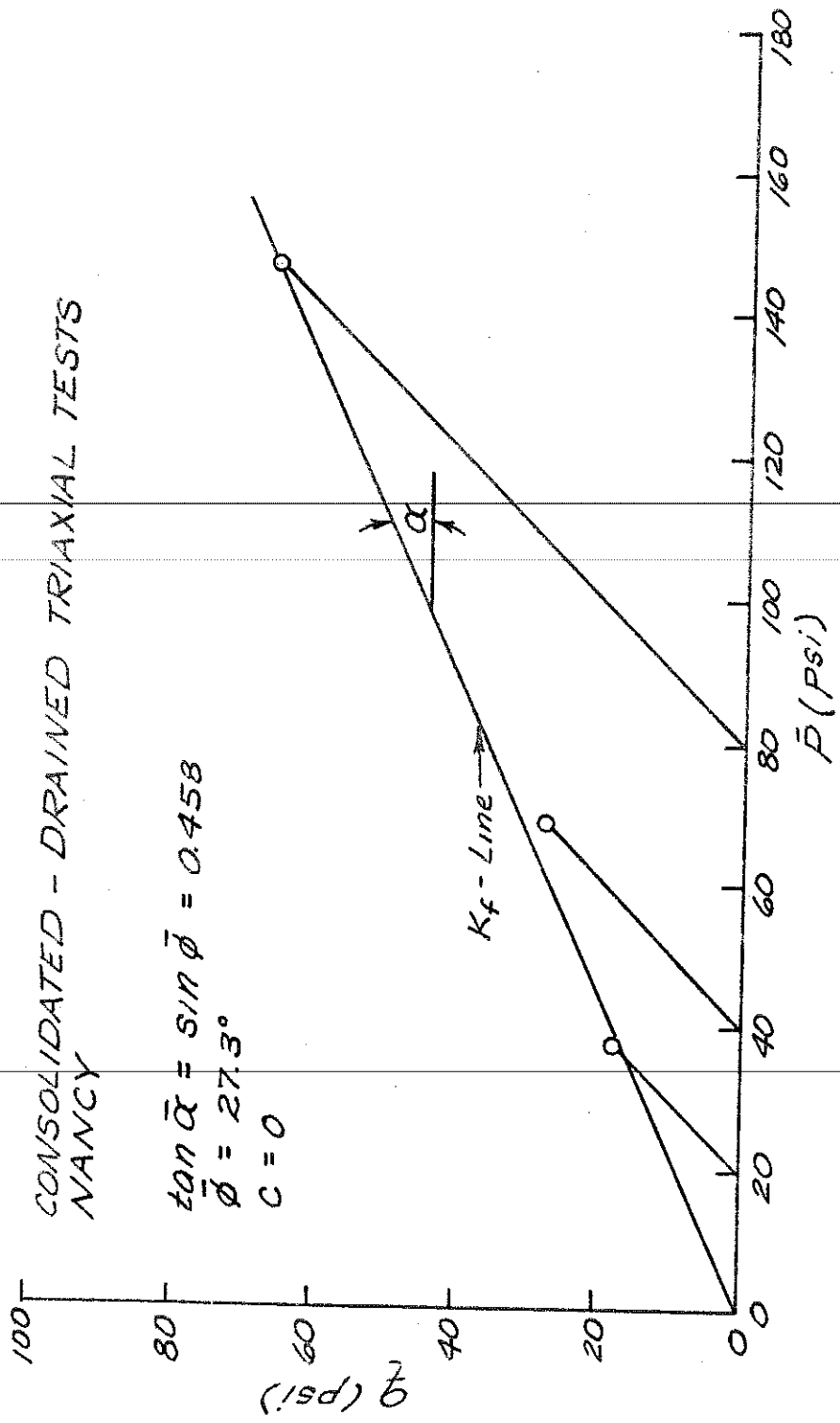


FIGURE 3. TRIAXIAL STRESS PATHS - NANCY.

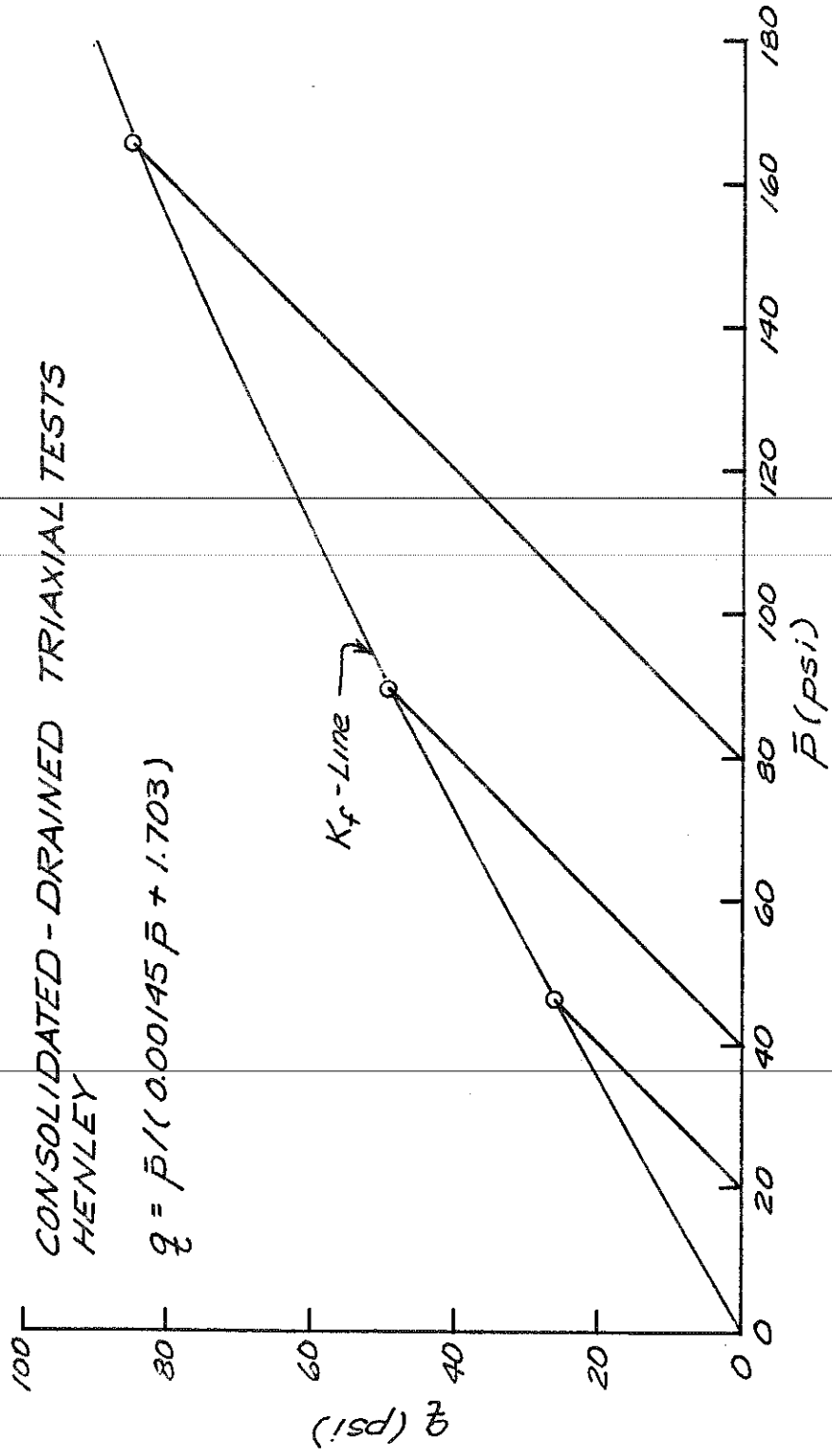


FIGURE 4. TRIAXIAL STRESS PATHS - HENLEY.

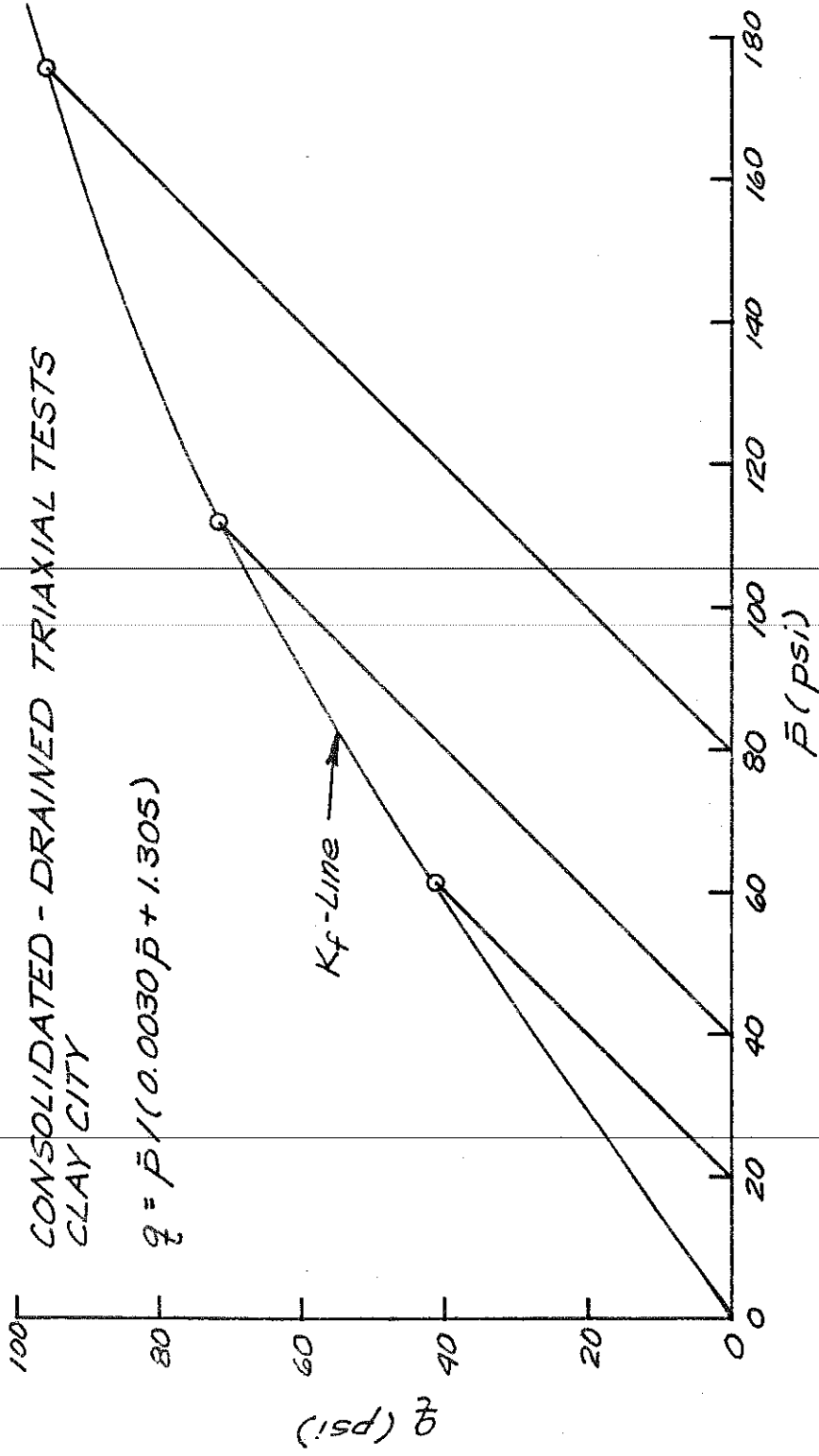


FIGURE 5. TRIAXIAL STRESS PATHS - CLAY CITY.



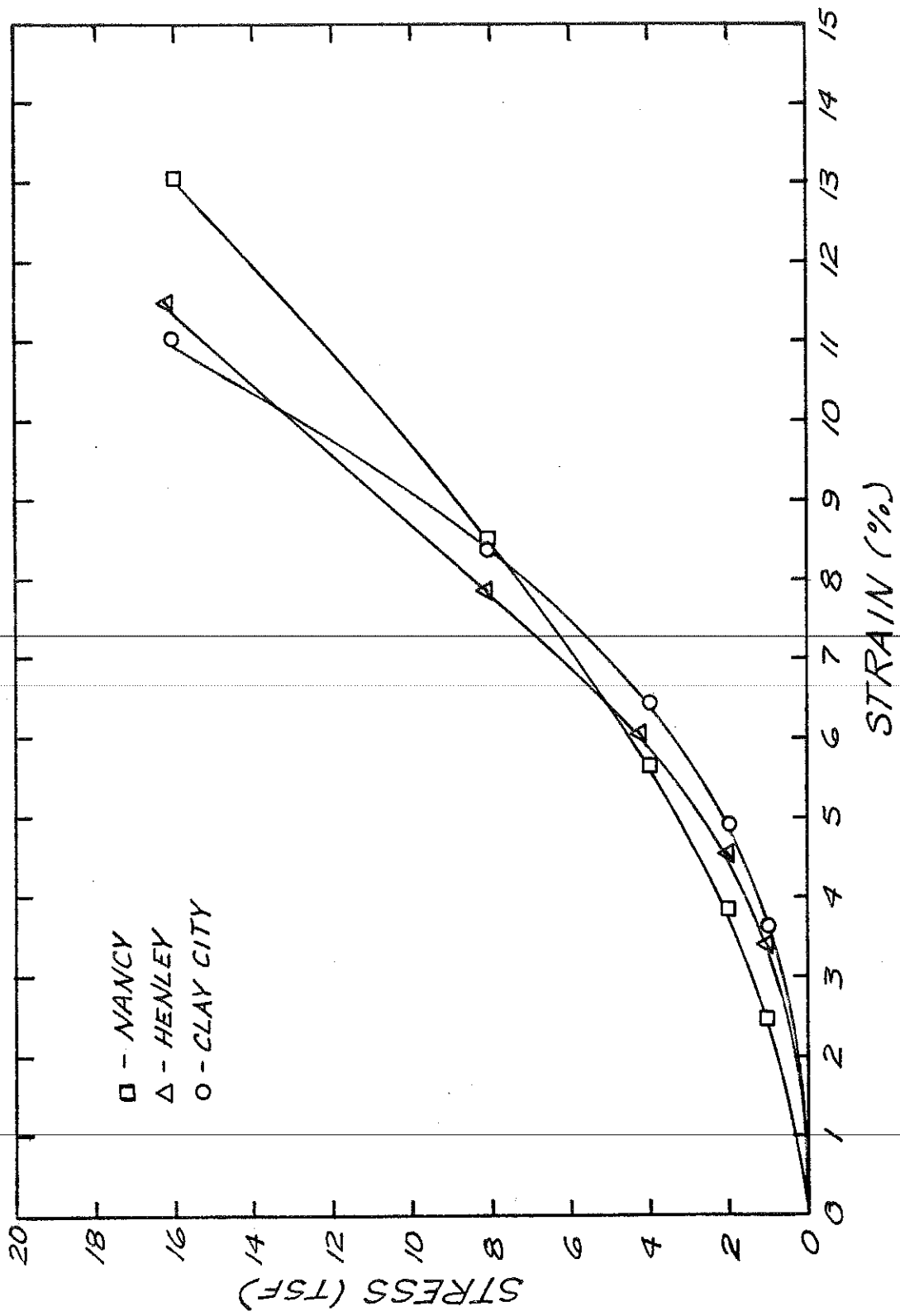


FIGURE 6. STRESS - STRAIN CURVES FOR ONE-DIMENSION COMPRESSION.

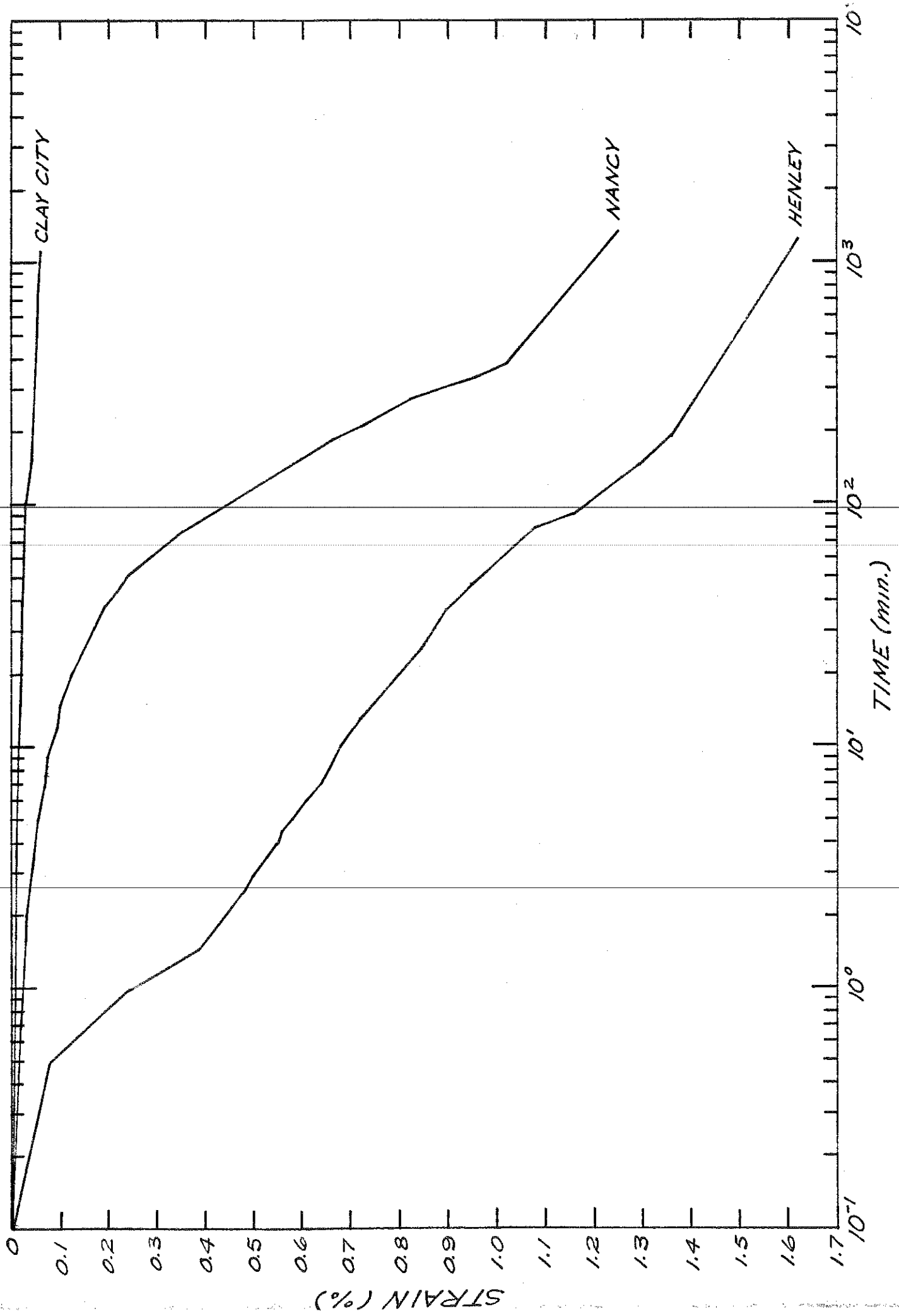


FIGURE 7. STRAIN-TIME CURVES FOR INUNDATED ONE-DIMENSIONAL COMPRESSION